

Supplemental Information

Effects of local symmetry on the upconversion emission mechanisms under pulsed excitation

Daniel Avram^a, Claudiu Colbea^a and Carmen Tiseanu^{*a}

^aNational Institute for Laser, Plasma and Radiation Physics, P.O. Box MG-36, RO 76900,
Bucharest-Magurele, Romania

Corresponding Author

* Author to whom correspondence should be addressed.

Electronic mail: carmen.tiseanu@inflpr.ro

Experimental details

Materials and characterization. The Er (Y) doped ZrO₂ nanoparticles were prepared by citrate complexation described elsewhere^{S1}. The 1% Er - ZrO₂ was calcined at 1000 °C and 1% Er, 3%Y - ZrO₂ was calcined at 850 °C (for 4 hours at a heating rate/cooling rate of 5 °C/min) to obtain pure monoclinic and tetragonal phase nanoparticles with similar crystallite size of 20 nm. An identical synthetical approach was used for 1% Eu, 3%Y - ZrO₂ and 1% Eu - ZrO₂. Powder X-ray diffraction (XRD) patterns were recorded on a Bruker-AXS D8 Advance diffractometer equipped with a one-dimensional detector (LynxEye type) using Cu-K α radiation (0.1541 nm) at a scanning speed of 0.04 degrees min⁻¹ in the 10 - 80 degrees 2 θ range with a collection time of 1s per step. The crystallite sizes were calculated from XRD patterns using Scherrer's Equation. Cell parameters were determined with MAUD software with its dedicated function based on the following formula $\frac{1}{d^2} = \frac{h^2+k^2}{a^2} + \frac{l^2}{c^2}$. Microbeam X-ray fluorescence (micro-XRF) spectrometry was performed on a custom-made instrument as described in Ref. ^{S2}. Attenuated total reflection-Fourier transform infrared (ATR-FTIR) spectra were measured on a Spectrum Two, PerkinElmer spectrometer using an ATR device with a diamond crystal plate (Pike Technologies, Madison, WI). Spectra were recorded at 4 cm⁻¹ nominal resolution and 100 scans. Raman analysis was carried out with a Horiba Jobin Yvon - Labram HR UV-Visible-NIR Raman. TEM characterization was performed using a Thermo Fisher Scientific Themis Z microscope equipped with Schottky field-emission electron gun operating at 300 kV and with both probe and image aberration-correctors.

Luminescence measurements. Time-resolved up-conversion emission spectra were recorded at room temperature using a wavelength tunable pulsed laser (210 ÷ 2300 nm), NT340 Series EKSPLA OPO (Optical Parametric Oscillator) as excitation source operated at 10 Hz with narrow bandwidth (around 5 cm⁻¹) and short pulse width (<5 ns) and for continuous-wave (cw) up-conversion emission, a 973 nm fiber coupled diode laser system (RLTMFC-980-4W-5, ROITHNER LASERTECHNIK GmbH) with a bandwidth of ~5 nm and ~8 W/cm² power density was used. As detection system, an intensified CCD (iCCD) camera (Andor Technology, iStar iCCD DH720) coupled to a spectrograph (Shamrock 303i, Andor) was used. Photoluminescence was detected with a spectral resolution of 0.44 nm and the input slit of the spectrograph was set to 10 μ m. For the emission spectra in the extended range of 500 - 1100 nm AvaSpec-HS1024x58/122TEC fiber coupled spectrometer was used. The Avantes spectrometer was calibrated by use of an integration sphere with a 5 W halogen bulb as calibration source, AvaSphere-50-LS-HAL-12V. In the

experiments, the same input slit (10 μm), exposure time (gate width of 0.5 ms), delay after the laser pulse (0.5 μs) and MCP gain (100) was used. The cw up-conversion emission spectra were recorded using the same input slit (10 μm) and exposure time (gate width of 100 ms). The powder samples were placed in the same geometrical configuration on a solid sample holder (sample holder area of 14 mm X 7 mm, from Horiba Scientific, J1933) in reflection mode using the same quantity of nanoparticles on all samples yielding the same excitation conditions (same energy density distribution on the samples) for comparison purposes. The UPC emission spectra represent the average of 5 spectra obtained with 1 nm incremental excitation around the measured excitation wavelength. The emission intensity was estimated as the integrated area from 500 to 750 nm or 500 to 1100 nm spectral range. All the digital photos were obtained by use of a Canon EOS 60D camera with 400 ISO and different integration time in dark room conditions.

For the visible emission decay measurements, a PMT module (PMA-C 192-N-M, PicoQuant GmbH) with appropriate filters and a PCIe TCSPC card TimeHarp 260 NANO (PicoQuant GmbH) as acquisition system was used for the near-infrared emission decay measurements, a NIR PMT module (H10330B-75, Hamamatsu) as detector coupled to a spectrograph/monochromator (Acton SP2758, Princeton Instruments) and a PCIe TCSPC card TimeHarp 260 NANO (PicoQuant) for acquisition was employed. The average decay lifetimes were estimated by integrating the area under the normalized emission decays: $\bar{\tau} = \int_0^{\infty} tI(t)dt / \int_0^{\infty} I(t)dt$, where $I(t)dt$ is the normalized decay law.

The UPC excitation spectra are measured using the protocol reported elsewhere⁵³. The time-resolved UPC excitation spectra (TREXS) were measured by scanning Er absorption around 980 nm (930 - 1000 nm) and 1530 nm (1400 – 1575 nm) using 1 nm step and laser energy kept constant at 5 mJ (71 mJ/cm²) and 3.15 mJ (45 mJ/cm²), respectively (see also Ref. ³). The time delays and gate widths varied from 0.0001 to 3 ms and 0.1 to 3 ms, respectively, depending on the time scale of the UPC emission. For each excitation wavelength, TREXS were constructed by integrating the area of the emission bands (550, 680 and 800 nm) measured at a specific delay after the laser pulse and gate-width. The time delays and gate widths were carefully selected considering the signal to noise ratio of transients and the comparison between the timescales of these under both upconversion and downconversion excitation modes.

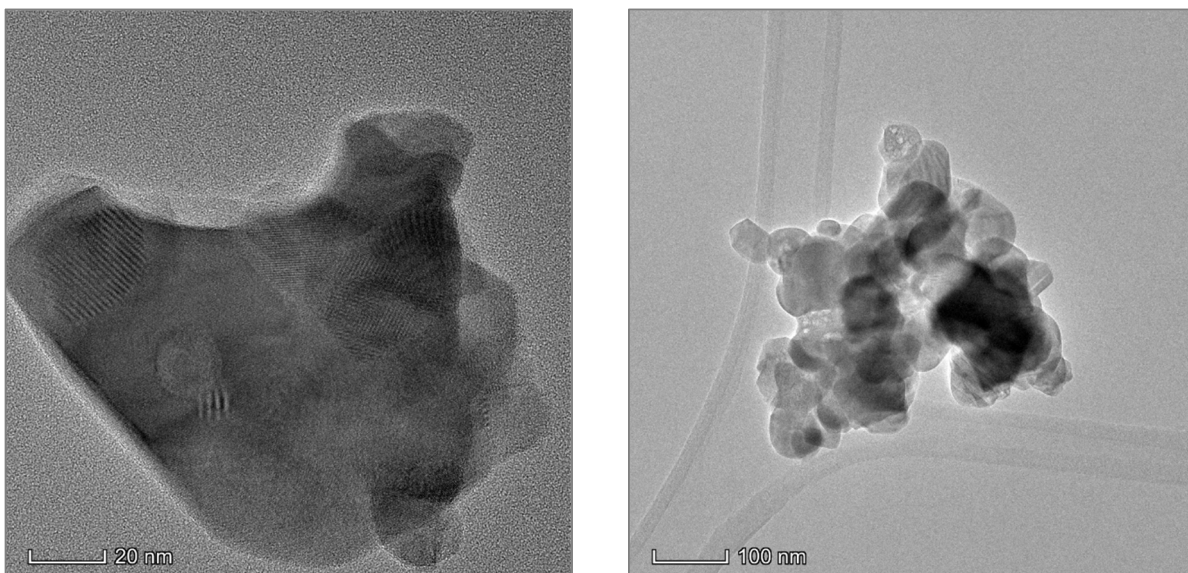


Figure S1. TEM images of $\text{Er} - \text{ZrO}_2(t)$ (left) and $\text{Er} - \text{ZrO}_2(m)$ (right) showing mild agglomeration of nanoparticles with heterogeneous morphology with sizes between 20 and 80 nm.

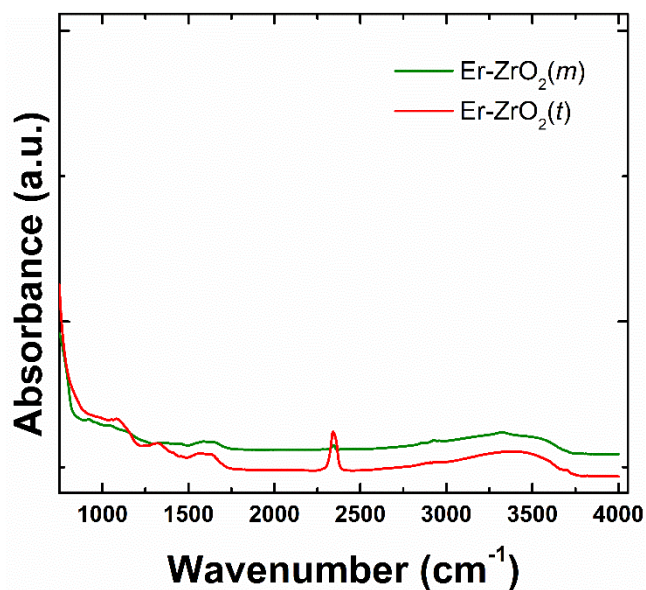


Figure S2. FTIR spectra of Er – ZrO₂(t) (left) and Er – ZrO₂(m)

Bands at $\sim 1630 \text{ cm}^{-1}$ (deformation vibration) or in the $3000 - 3600 \text{ cm}^{-1}$ (stretching vibration) region corresponding to OH bond, indicating the presence of coordinated or adsorbed water, respectively. It should be noted that, although the tetragonal sample was annealed at a lower temperature than the monoclinic sample, its upconversion intensity is comparable (around 980 nm excitation) and up to two orders of magnitude more intense (around 1530 nm excitation); in other words, equal anneal temperatures would strengthen even more the trend observed but at the cost of getting different particle sizes.

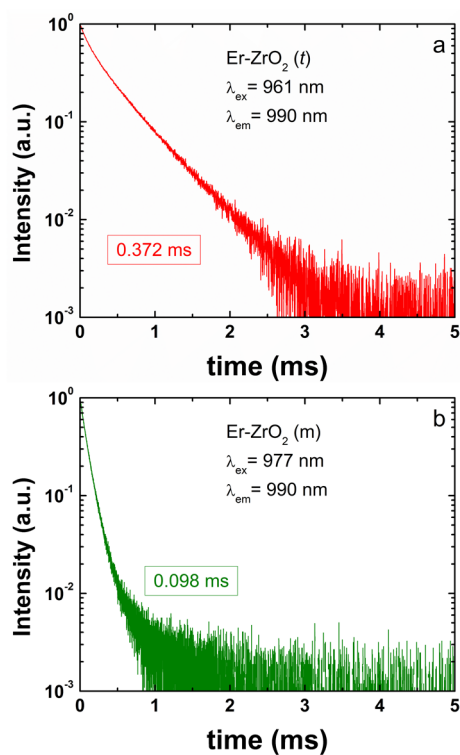


Figure S3. Comparison between the emission decays of $^4I_{11/2}$ level of Er – ZrO₂(t) (a) and Er – ZrO₂(m) (b) under direct excitation (DC) at 961 and 977 nm.

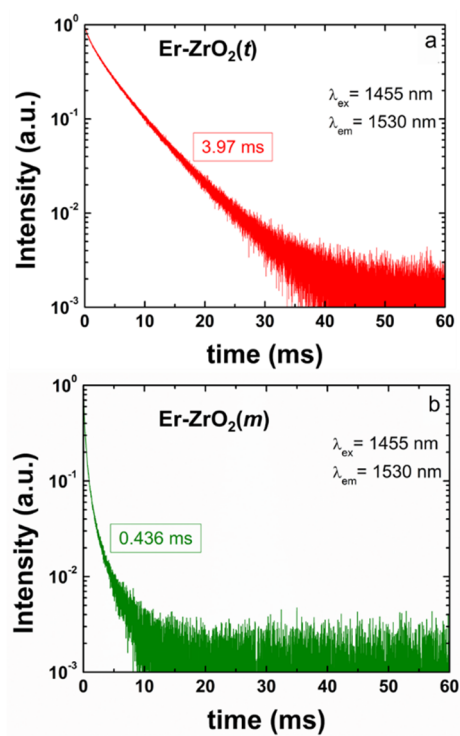


Figure S4. Comparison between the emission decays of $^4I_{13/2}$ level of $\text{Er-ZrO}_2(t)$ (a) and $\text{Er-ZrO}_2(m)$ (b) under direct excitation (DC) at 1455 nm.

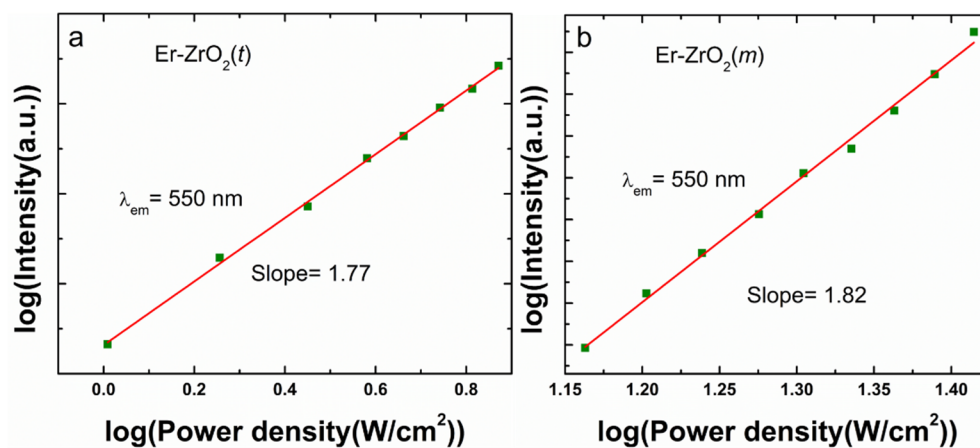


Figure S5. The dependence of up-conversion emission intensity of $\text{Er-ZrO}_2(t)$ and $\text{Er-ZrO}_2(m)$ on the pump power density upon excitation at 973 nm (emission was monitored at 550 nm) confirming that the green emission is induced by 2nd order process.

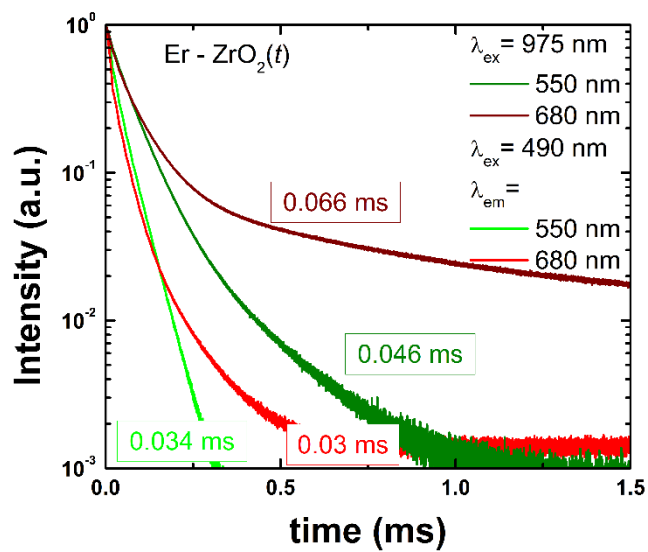


Figure S6. The emission decay monitored at 550 and 680 nm under 490 (DC) and 975 nm (UPC) excitation for Er – ZrO₂(t). The emission decays were constructed using time-resolved emission spectra.

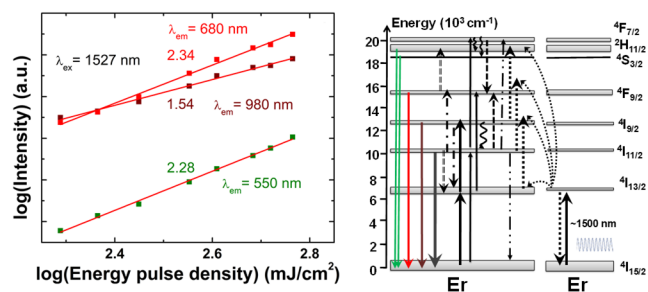


Figure S7. Energy density dependencies of upconversion emission intensity monitored at 550, 680 and 980 nm excited at 1530 nm (left). Scheme with relevant transitions involved in upconversion emission of $\text{Er-ZrO}_2(t)$ (right).

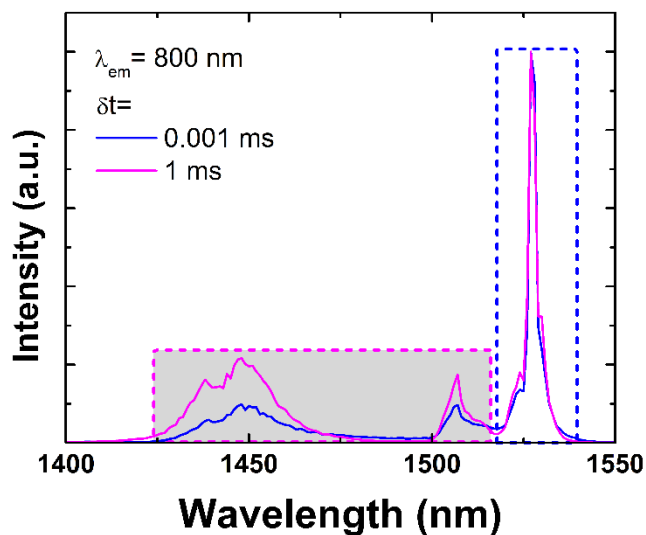


Figure S8. Time-resolved UPC (TREXS) spectra of Er-ZrO₂(t) monitored at 800 nm (corresponding to ⁴I_{9/2}-⁴I_{13/2}) excited in the 1400 - 1550 nm spectral range. TREXS displays an enhanced spectral dynamic as the integrated area varies from 7.5 (at 0.001 ms delay) to 10.7 (at 1 ms delay), likely because this level is efficiently populated by a two-photon ground state/excited state absorption.

References

- S1. Fuentes, R.; Baker, R., Synthesis of Nanocrystalline CeO₂-ZrO₂ Solid Solutions by a Citrate Complexation Route: A Thermochemical and Structural Study. *Journal of Physical Chemistry C* **2009**, *113* (3), 914-924.
- S2. Lungu, M.; Dobra, C.; Craciunescu, T.; Tiseanu, I.; Porosnicu, C.; Jecu, I.; Mustata, I., Mixed film coatings analyzed by micro x-ray fluorescence method. *Digest Journal of Nanomaterials and Biostructures* **2014**, *9* (3), 899-906.
- S3. Tiseanu, C.; Parvulescu, V.; Avram, D.; Cojocaru, B.; Apostol, N.; Vela-Gonzalez, A.; Sanchez-Dominguez, M., Structural, down- and phase selective up-conversion emission properties of mixed valent Pr doped into oxides with tetravalent cations. *Physical Chemistry Chemical Physics* **2014**, *16* (12), 5793-5802.